

1 **Title:** Differential effects of emotional valence on mnemonic performance with greater hippocampal matu-
2 rity

3 **Abbreviated title:** Effects of valence on memory performance with hippocampal maturity

4 **Author Names and Affiliations:** Adam Kimbler¹, Dana McMakin^{1,2,4}, Nicholas J. Tustison³, Aaron T.
5 Mattfeld^{1,4}

6 ¹: Cognitive Neuroscience Program, Department of Psychology, Florida International University, Miami, FL 33199

7 ²: Clinical Neuroscience Program, Department of Psychology, Florida International University, Miami, FL 33199

8 ³: Department of Radiology and Medical imaging, University of Virginia, Charlottesville, VA 22903

9 ⁴: Center for Children and Families, Florida International University, Miami, FL 33199

10 **Corresponding Author:** Aaron T. Mattfeld (amattfel@fiu.edu)

11 **Number of pages:** 26

12 **Number of figures:** 6

13 **Number of Words:**

14 • **Abstract:** 249

15 • **Significance Statement:** 114

16 • **Introduction:** 650

17 • **Discussion:** 1302

18 **Conflict of interest statement:** The authors declare no competing financial interests.

19 **Acknowledgements:** None

20 **Abstract**

21 The hippocampal formation (HF) facilitates the creation of declarative memories, with subfields providing unique
22 contributions to the discriminability and generalizability of events. The HF itself and its connections with other struc-
23 tures exhibit a protracted development. Maturation differences across subfields facilitate a shift towards memory
24 specificity, with peri-puberty sitting at the inflection point. Peri-puberty also happens to be a sensitive period in the de-
25 velopment of anxiety disorders. Taken together, we believe HF development is critical to negative overgeneralization,
26 a common feature of anxiety disorders. To investigate the role of the HF in behavioral discrimination and general-
27 ization we examined the relation between behavior and cross-sectional indices of HF maturity derived from subfield
28 volume. Participants aged 9-14 years, recruited from clinical and community sources, performed a recognition task
29 with emotionally valent (positive, negative) and neutral images. T1-weighted and diffusion-weighted structural scans
30 were collected. Partial least squares correlations were used to derive a singular metric of maturity for both HF volume
31 and structural connectivity. We found our volumetric HF maturity index was positively associated with discrimi-
32 nation for neutral images and generalization for negative images. Hippocampal-medial prefrontal cortex structural
33 connectivity maturity metric evidenced a similar trend with behavior as the HF volumetric approach. These findings
34 are important because they reflect a novel developmentally related balance between discrimination and generalization
35 behavior supported by the hippocampus and its connections with other regions. Maturation shifts in this balance
36 may contribute to negative overgeneralization, a common feature of anxiety disorders that escalates during the same
37 developmental window.

38 **Significance Statement**

39 The hippocampal formation (HF) facilitates declarative memory specificity and is composed of subfields whose de-
40 velopment during adolescence overlaps with the onset of anxiety disorders. Aberrations in mechanisms governing
41 memory specificity may contribute to negative overgeneralization in anxious youth. Participants completed an emo-
42 tional memory discrimination task while in the scanner. Using a multivariate maturity metric based on subfield volume
43 we found individuals with more “mature” HF were better at differentiating similar neutral images and more likely to
44 generalize similar negative images. These findings are important because they capture a novel developmental mech-
45 anism related to the balance between discrimination and generalization. Shifts in this balance, may contribute to
46 negative overgeneralization, a common feature of anxiety disorders.

47 **Introduction**

48 Memory increases in specificity, driven by maturation of key neurobiological substrate taking root around the onset of
49 puberty and continuing into adolescence (Lavenex et al., 2007; Lee et al., 2014; Daugherty et al., 2017; Keresztes et al.,
50 2018). Whether these specificity-supporting neurobiological mechanisms are similarly employed across different stim-
51 ulus valences (e.g., emotional versus neutral) remains under-specified. Around the same developmental window, the
52 prevalence of anxiety disorders increases (Beesdo et al., 2009). Together, understanding how developmental changes
53 in memory specificity interact with emotional salience of stimuli may provide important insight into our understanding
54 of negative overgeneralization, a characteristic symptom of anxiety where individuals generalize negative associations
55 to similar events (Lissek et al., 2014). In the current study, we aim to understand the relation between cross-sectional
56 indices of neurobiological maturation around the onset of adolescence and measures of behavioral discrimination and
57 generalization to stimuli with emotional valence.

58 A network of interconnected regions in the medial temporal lobe (MTL) and medial prefrontal cortex (mPFC) govern
59 the specificity of declarative memories. The MTL is comprised of the rhinal cortices, the amygdala, and the hippocam-
60 pal formation (HF) (Squire et al., 2004). The HF can be further separated into distinct subfields: dentate gyrus (DG),
61 Cornu Ammonis (CA) 1, 2, and 3, and subiculum. In human neuroimaging studies, the DG and CA3 subfields are
62 often combined due to difficulties in reliably separating them (Daugherty et al., 2017). The amygdala is comprised of
63 the central, medial, lateral, and basolateral complex nuclei (Phelps and LeDoux, 2005). Unique functional attributes
64 are conferred by underlying architecture (Marr, 1971; Rolls, 2001) and connectivity (Ranganath et al., 2004; Gold-
65 stein et al., 2009; Bennett and Stark, 2016) of the MTL and mPFC. For example, the DG plays a disproportionate
66 role in ‘pattern separation’ given its high number of granule cells and sparse firing, while the recurrent collaterals
67 of the CA3 facilitate ‘pattern separation’ (Yassa and Stark, 2011; Rolls, 2013; Knierim and Neunuebel, 2016). The
68 amygdala, contributes to the encoding of emotional salience of stimuli and events (McGaugh and Ayala, 2013) and the
69 subsequent modulation of memory (McGaugh, 2004) with damage selectively impairing gist or generalized memories
70 (Adolphs et al., 2001, 2005). While, the mPFC interacts with both the amygdala and HF regulating memory specificity
71 (Colgin, 2011; Xu and Südhof, 2013; Jin and Maren, 2015; Sekeres et al., 2018).

72 Notably, the HF and mPFC are characterized by prolonged developmental trajectories extending well into adulthood
73 with particularly rapid changes occurring around the onset of adolescence (Giedd et al., 1996; Lavenex and Banta
74 Lavenex, 2013; DeMaster et al., 2014; Avino et al., 2018). Moreover, the distinct developmental trajectories have
75 been shown to differentially impact behavior (Lee et al., 2014; Keresztes et al., 2018; Riggins et al., 2018). However,
76 cognition does not emerge from the independent contributions of individual brain regions but rather reflects the prod-

77 uct of networks of brain regions interacting (McIntosh, 2000). Thus, developmentally related increases in memory
78 specificity likely reflect the composition of maturational changes across regions rather than the contribution of single
79 regions alone (Keresztes et al., 2018).

80 To examine the role of MTL maturity on discrimination and generalization of stimuli with emotional valence in a
81 sample of peri-pubertal youth, participants completed an emotional similarity task (Leal et al., 2014) where they
82 rated the valence of stimuli (negative, neutral, positive) during a Study session in the scanner, then returned to the
83 scanner after 12 hours for a surprise memory test where they made ‘old’ or ‘new’ judgments. Separate volumetric
84 and connectivity based HF and amygdala maturity were assessed using a partial least squares correlation analysis
85 (PLSC) using the structural and diffusion weighted scans (Keresztes et al., 2017, 2018). Behavioral measures of both
86 discrimination and generalization were related to the multivariate measures of volume and connectivity. We tested
87 the hypothesis that emotional valence of stimuli differentially produced increasing neutral discrimination and negative
88 generalization with increasing hippocampal and amygdala maturity.

89 **Methods**

90 **Participants**

91 Fifty-two peri-pubertal youth (age 9-14 years) were recruited from mental-health clinics and the Miami-Dade commu-
92 nity for a larger study to examine the neurobiological correlates of negative overgeneralization (McMakin et al., 2020).
93 A strategy of recruiting from anxiety clinics and the community was used to maximize variability in key dimensions
94 of interest—generalization and discrimination of emotional stimuli. Youth with anxiety are known to experience wide
95 generalization gradients to negative stimuli in particular (Greenberg et al., 2013), which clinically appears as a ten-
96 dency to pathologically extend fear from aversive contexts (e.g. house fire) to safe contexts with shared features (e.g.
97 campfire). Participants recruited for the study were assessed for medical and psychiatric exclusionary criteria (e.g.,
98 current depressive episode, bipolar disorder, post-traumatic stress disorder, conduct disorder, oppositional defiant dis-
99 order, psychotic disorders, and obsessive-compulsive disorder) based on a screener assessing key symptoms associated
100 with DSM-IV diagnoses and/or a parent-reported diagnosis. Following intake, three participants were ineligible for
101 the study (left-handed) and another dropped out, leaving 48 volunteers to participate in the Study session scan. Two
102 participants were not invited for the Test session scan due to excessive movement and an error in the experimental
103 paradigm. A third participant failed to show-up for their appointment leaving 45 participants who completed the Test
104 session scan. Eleven participants were excluded following the Test session: one failed to show up to their appointment,
105 six for poor performance (hit rate for targets was 1.5SD below the average performance), three for errors in triggering
106 the onset of the scanner with the task, and one participant was removed for excessive motion during the scan (defined

107 as greater than 0.5mm of framewise displacement for more than 30% of volumes) leaving 34 participants (11.4 ± 2.0
108 years, 16 female) in the final sample. All participants provided written informed consent (legal guardian) and assent,
109 and were compensated for their time.

110 Behavioral Procedures and Methods

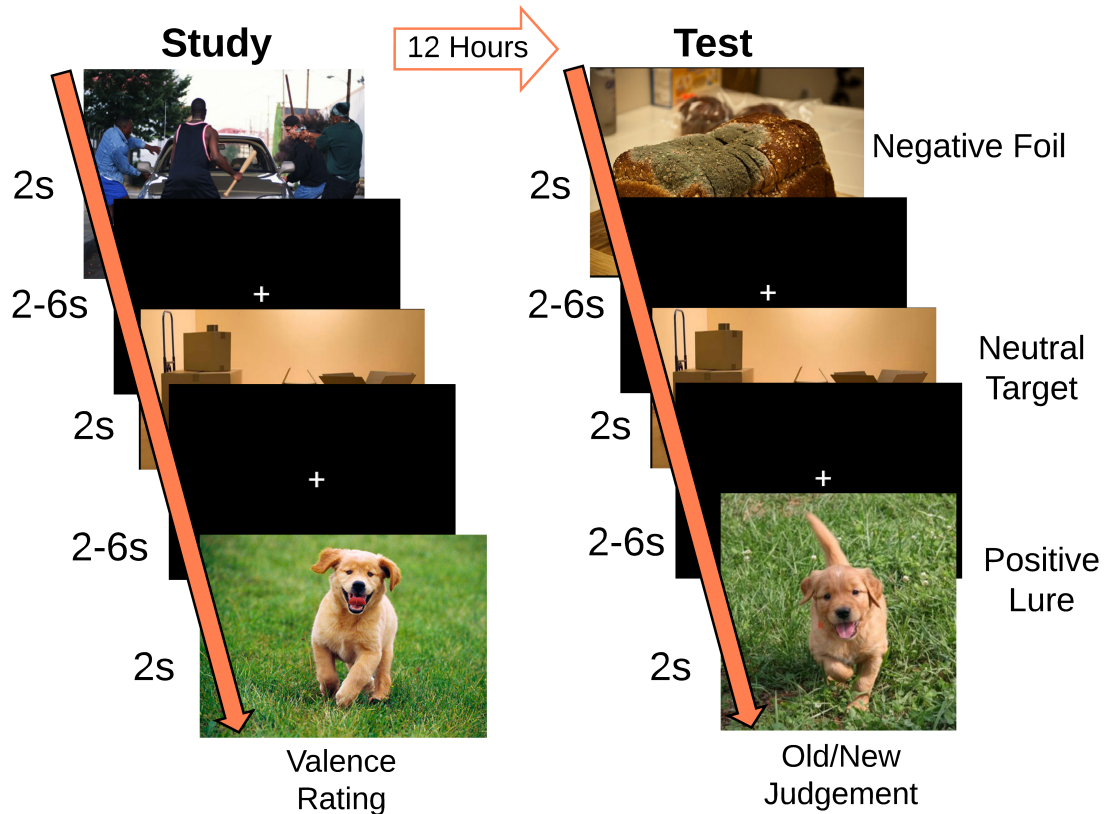


Figure 1. Trial structure of emotional similarity task. Participants experienced two scanning sessions. The Study session consisted of 145 images of differing valences while the Testing session consisted of a recognition memory task comprised of 284 images across the three valences with Targets (presented during the Study session), Foils (new images), and Lures (stimuli similar to the items presented during the Study session).

111 Participants took part in an emotional similarity task (Fig. 1). The task included an incidental encoding session during
112 which participants viewed scenes (2000 ms) and were instructed to endorse images as either: negative, neutral, or
113 positive. Stimuli were separated by a jittered inter-stimulus-interval (2000-6000 ms) during which a white central
114 fixation was presented on a black background. Each scene was presented once, totaling 145 images (48, negative, 47
115 neutral, 50 positive). Participants returned 12 hours later for a surprise memory test, with approximately half ($n=16$) of
116 them performing the task in the morning, post-sleep. During the Test session, participants were instructed to endorse

117 images as either ‘old’ or ‘new.’ A total of 284 images were presented: forty-eight targets (16 each of negative, neutral,
118 and positive) – repetitions of the images presented during the incidental encoding session; ninety-seven (32 negative,
119 32 neutral, and 33 positive) lures – images similar to but not exactly the same as an image shown during the incidental
120 encoding session; and 139 foils (42 negative, 49 neutral, 48 positive) – images never presented before and not sharing
121 similarity to the original images. Participants were asked to indicate whether each image was either ‘old’ (the subject
122 recalls seeing that exact image during the Study session) or ‘new.’ They were instructed to endorse images as ‘old’
123 only if they were the exact same as the image seen during the Study session and to respond while the image was still
124 on the screen. During the Test session each image was also presented for 2000 ms.

125 A lure generalization index (LGI) was calculated for each image valence by subtracting the proportion of old responses
126 when given a foil image from the proportion of old responses when given a lure image (1).

$$LGI = p('old'|Lure) - p('old'|Foil) \quad (1)$$

A lure discrimination index (LDI) was calculated for each valence by subtracting the proportion of new responses to
targets from the proportion of new responses to lures (2).

$$LDI = p('new'|Lure) - p('new'|Target) \quad (2)$$

127 **Neuroimaging Data Collection and Preprocessing**

128 Neuroimaging data were collected on a 3T Siemens MAGNETOM Prisma scanner with a 32-channel head coil at the
129 Center for Imaging Science at Florida International University. Diffusion-weighted images (1.7mm isotropic) using
130 a multiband sequence (slice acceleration factor=3, 96 directions, seven b=0 frames, and four b-values: 6 directions
131 with 500s/mm², 15 directions with 1000s/mm², 15 directions with 2000s/mm², and 60 directions with 3000s/mm²) in
132 addition to a T1-weighted magnetization-prepared rapid gradient echo sequence (MPRAGE: TR=2500ms, TE=2.9ms,
133 flip angle=8°, FOV=256mm, 176 sagittal slices, voxel size=1mm isotropic) were collected. A fieldmap opposite of the
134 phase encode direction of the dMRI acquisition was also acquired for distortion correction.

135 FreeSurfer’s (version 6.0.0; Fischl, 2012) ‘recon-all’ algorithm was applied to each participant’s T1-weighted struc-
136 tural scan to obtain cortical surface reconstruction and cortical/subcortical segmentations. For diffusion image prepro-
137 cessing, each participant’s diffusion weighted scan was registered to FreeSurfer structural space using boundary-based
138 registration with the reference image being the first acquired b=0 frame. The FreeSurfer parcellation and segmentation
139 file (aparc+aseg) was then binarized and transformed into diffusion space using FreeSurfer’s ‘ApplyVolTransform’ tool

140 and was then binarized and dilated by 1mm to include edge voxels to act as a brain mask. Susceptibility distortion
141 correction was then performed using FSL Topup, followed by eddy current correction using FSL Eddy on the diffusion
142 data masked by the dMRI space brain mask. This preprocessed data was then input in to FSLs BEDPOSTX (Jbabdi et
143 al., 2012) to model crossing fibers within each brain voxel. The results of BEDPOSTX were the basis of all subsequent
144 probabilistic tractography based analyses.

145 **Delineating Amygdala Subregions**

146 The amygdala is comprised of several nuclei, with each having unique anatomical connections to cortical and sub-
147 cortical targets. We used probabilistic tractography combined with a novel method of k-means clustering analysis to
148 identify amygdala subregions. Probabilistic tractography was computed from bilateral masks of the amygdala to 24
149 ipsilateral cortical and subcortical targets while avoiding the ventricles. This resulted in separate files (one for each
150 target) containing the total number of random walks completed from each voxel in the amygdala mask to that specific
151 targets. Each file was then vectorized and included in an $n \times m$ array, with n being the number of voxels in the left or
152 right amygdala masks, and m being the number of amygdala targets. The array was then subjected to a k-means clus-
153 tering algorithm with a limit of 4 clusters, with voxels serving as samples and targets serving as features, implemented
154 in Python (scikit-learn). Each voxel in the amygdala masks were assigned a k-means cluster value based on their
155 connectivity across the targets (aka, features), which were then coerced back into their three-dimensional anatomical
156 representations. Volume estimates were then extracted for each of these clusters while correcting for ICV (Fig. 2).

157 **Delineating Hippocampal and Cortical Regions of interest (ROI)**

158 Hippocampal subfields (bilateral DG/CA3, CA1, and subiculum) and the posterolateral and anteromedial entorhinal
159 cortices were segmented using a consensus labeling approach. First, manual segmentations (Yassa and Stark, 2009;
160 Yushkevich et al., 2015) were applied to an atlas set of 19 T1 MPRAGE scans and their corresponding T2-FSE scans
161 (oblique orientation perpendicular to the long axis of the hippocampus; 0.47 mm² in -plane, 2.0 mm slice thickness).
162 Weighted consensus labeling from the atlas to an unlabeled T1 was accomplished by normalizing the atlas set to the
163 unlabeled subject and applying multi-atlas segmentation with joint label fusion (Wang and Yushkevich, 2013). This
164 approach capitalizes on both label and intensity information and has been used in a number of recent publications to
165 segment hippocampal subfields (Sinha et al., 2018; Brown et al., 2019) (Fig. 3A). Cortical ROIs (e.g., perirhinal cortex,
166 parahippocampal cortex, amygdala, superior frontal cortex, caudal and rostral anterior cingulate cortex, and medial
167 orbitofrontal cortex) were created by binarizing FreeSurfer segmentations. All volume estimates were corrected for
168 intercranial volume and age by multiplying each volume estimate by the ratio of age predicted whole-brain volume to
169 actual whole-brain volume obtained via FreeSurfer .

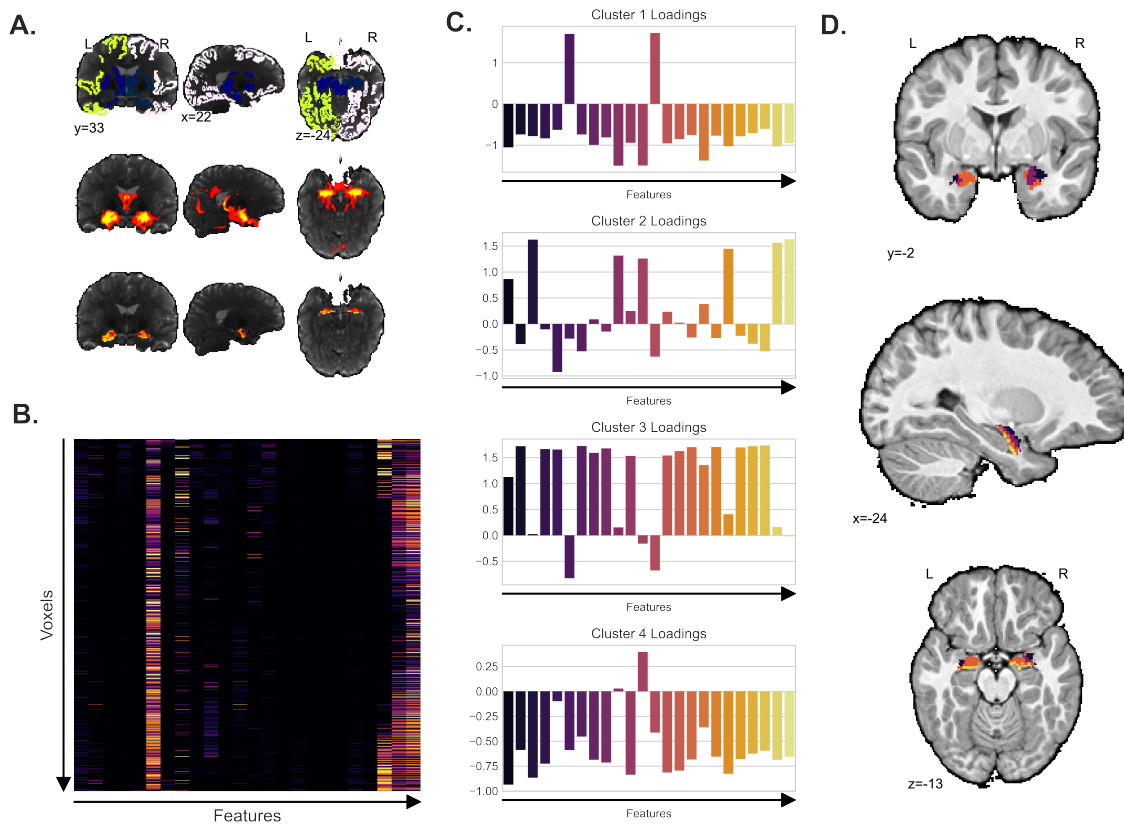


Figure 2. Delineation of the Amygdala through k-means clustering. (A) Probabilistic Tractography from the amygdala to 26 ipsilateral cortical and subcortical targets (first row) allowed for the definition of fiber pathways (second row) which allowed for the construction of metrics of anatomical connectivity in the form of number of walks to the target (third row; pictured is the number of successful walks from the amygdala to the HF). (B) From the random walk data, a matrix of number of random walks from amygdala to target was constructed across voxels in the amygdala. (C) The correlation matrix was then placed into a k-means clustering algorithm implemented in ‘scipy’ set to sort the data into 4 clusters, with cluster loadings pictured. (D). These four clusters were then classed for each participant, with an exemplar pictured.

170 Measures of Regional Connectivity

171 To examine the structural connectivity between regions, probabilistic tractography was conducted using FSL’s Prob-
172 trackx (Behrens et al., 2003, 2007) with 25,000 streamline samples (step length=0.5, curvature threshold=0.2, maxi-
173 mum steps=2000) in each seed voxel to produce a connectivity distribution between each seed and target region, while
174 avoiding paths through the ventricles. A list of the connections examined appears in Table 1.

Table 1. Seeds to target regions for connectivity analyses

Connection	Seed Region	Target Regions
Amygdala to HF	Amygdala	DG/CA3, CA1, ERC, Subiculum
HF to Rhinal	HF	PRC, pHPC, Posterior mERC, Anterior lERC
HF to mPFC	HF	Caudal ACC, Rostral ACC, Superior Frontal, mOFC

175 **Regional Volumetric Maturity Estimates using PLSC**

176 To calculate regional maturity scores partial least squares correlation (PLSC) was conducted to produce regional maturity for the HF (DG/CA3, CA1, subiculum, posterolateral and anteromedial entorhinal cortices), rhinal (RHI) cortices (posterolateral and anteromedial entorhinal cortices, perirhinal cortex, and parahippocampal cortex), and amygdala (AMY) (resulting k-means clusters determined by probabilistic tractography) according to an approach first outlined by [Keresztes et al. \(2017\)](#). A correlation matrix was produced by correlating AGE (in months) and volumetric measures for each ROI. The resultant matrix was then decomposed via singular value decomposition (SVD). Resultant weights for each ROI were then multiplied by each subject's vector of ROI volumes to produce a singular regional maturity score. This process was completed for the HF, RHI and AMY to produce Hippocampal, Amygdala, and Rhinal Maturity Scores respectively.

185 **Connectivity Maturity Estimates using PLSC**

186 PLSC was also used to compute connectivity maturity metrics between regions. A correlation matrix was constructed using AGE (in months) and the median number of random walks between the seed and target regions. This matrix was decomposed via SVD and the resultant weights were multiplied by the median connection strength to produce a connectivity maturity score. This was conducted for all connections outlined in [Table 1](#). (Amygdala to HF, HF to Rhinal Cortices, and HF to mPFC).

191 **Statistical Analyses**

192 Analyses into the effects of maturity and valence on lure generalization and discrimination outcomes were conducted using linear mixed-effects modeling conducted using the 'lme4' package in R version 3.6.1 ([Bates et al., 2015](#)). In this model valence and maturity were entered as predictors, and subject was modeled as the random intercept. Interactions were probed using simple-effects analysis also conducted in R.

196 **Results**

197 **Hippocampal maturity was related to differential discrimination and generalization of neu-** 198 **tral and negatively valenced scenes**

199 To test our hypothesis that negative and neutral images experience different patterns of mnemonic discrimination and
200 generalization with multivariate volumetric hippocampal maturity during the emotional similarity task we examined
201 the association between individual's HF maturity scores with their discrimination and generalization performance
202 across image valence. Lure Discrimination and Lure Generalization Index (LDI and LGI respectively) scores were
203 calculated (Equations 1 and 2) to assess a participant's likelihood to discriminate or generalize lure stimuli, thought to
204 be dependent neurobiologically on pattern separation and completion respectively. As multiple models are present in
205 the current study, a Holm-Sidak corrected alpha of .026 was used to assess significance.

206 We observed differential patterns in the discrimination and generalization of emotionally valent lure stimuli across
207 our HF maturity scores. As predicted, when comparing negative and neutral stimulus discrimination (e.g., LDI) we
208 identified a significant interaction between HF maturity and stimulus valence ($maturity*valence : F(1, 32) = 6.159$,
209 $p = .019$, $R^2 = .161$), with greater discrimination of neutral images associated with elevated HF maturity scores
210 ($\beta = .033$, $CI(95) = (0.003, 0.072)$, $t(33) = 2.244$, $p = .032$), while discrimination of negative images showed no
211 evidence of such relationship with HF maturity ($\beta = .016$, $CI(95) = (-0.041, 0.034)$, $t(33) = -0.472$, $p = .640$)
212 (Fig. 3B). When assessing generalization (e.g. LGI) we similarly observed divergent patterns between negative and
213 neutral stimuli ($maturity * valence : F(1, 32) = 5.737$, $p = .023$, $R^2 = .126$). We found enhanced generalization
214 of negative images associated with greater HF maturity scores ($\beta = .030$, $CI(95) = (0.003, 0.057)$, $t(33) = 2.324$,
215 $p = .027$) while neutral generalization did not differ as a function of our HF maturity measure ($\beta = -.000$, $CI(95) =$
216 $(-0.023, 0.019)$, $t(33) = -0.054$, $p = .957$) (Fig. 3C)

217 **Valence related differences in discrimination and generalization not observed in the rhinal** 218 **cortices or amygdala**

219 To assess the specificity of the observed interactions with discrimination and generalization of emotionally valent
220 images and our HF maturity scores, we probed for similar associations between maturity and emotional valence
221 in neighboring MTL regions; such as the rhinal cortices and amygdala, two regions anatomically connected to the
222 hippocampus (Suzuki and Amaral, 1994) and important for memory and emotional processing (McGaugh, 2004), with
223 the rhinal cortices experiencing earlier development than both the amygdala and HF (Insausti et al., 2010). We did
224 not observe divergent patterns in discrimination (LDI) across our multivariate maturity measures and image valence

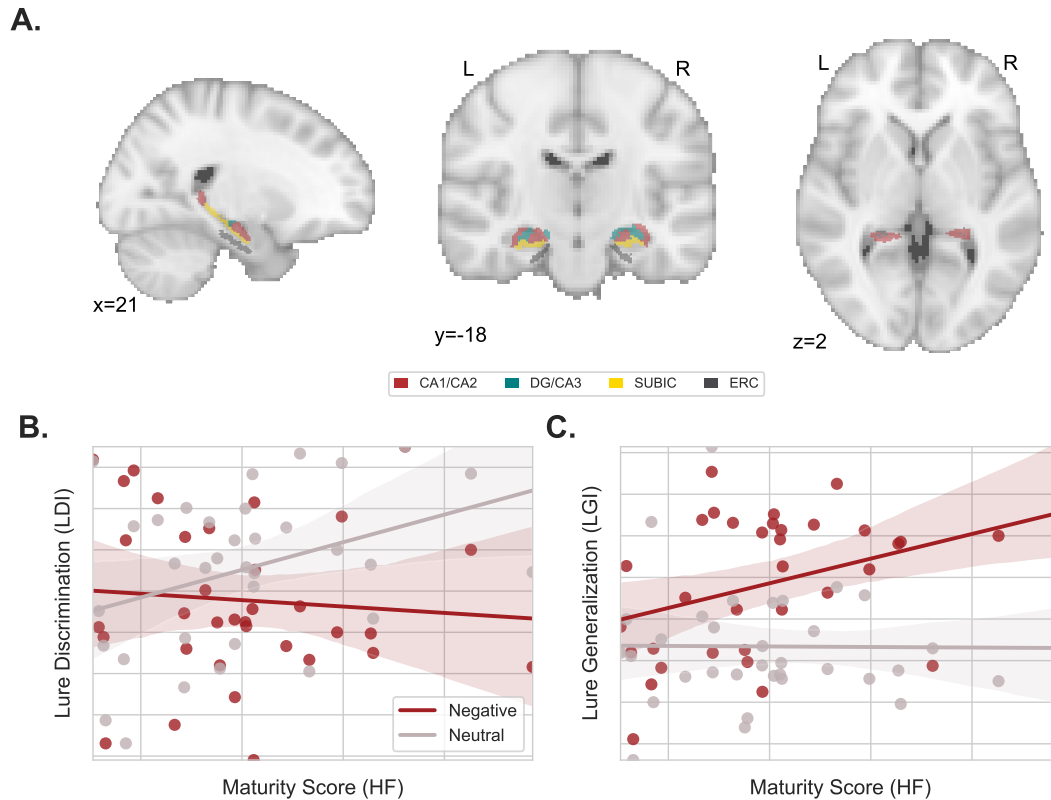


Figure 3. Differential relation between hippocampal maturity and memory performance across stimulus valence. (A) Hippocampal subfield volume estimates from the CA1/CA2, DG/CA3, Subiculum and entorhinal cortices (ERC) were used to produce a metric of hippocampal maturity as in Keresztes et al. (2017). (B) There was a significant interaction between image valence and hippocampal maturity predicting LDI performance ($maturity * valence : F(1, 32) = 6.159, p = .019, R^2 = .161$), with negative LDI showing no evidence of change across different levels of hippocampal maturity while neutral LDI performance increased. (C) An opposing significant interaction appeared for LGI performance ($maturity * valence : F(1, 32) = 5.737, p = .023, R^2 = .126$) where negative LGI increased across hippocampal maturity, whereas neutral LGI showed no evidence of change.

225 in the rhinal cortices ($maturity * valence : F(1, 32) = 0.000, p = 0.986$) or the amygdala ($maturity * valence :$
226 $F(1, 32) = 1.185, p = 0.284$) (Fig. 4A,C); nor divergent generalization (LGI) across maturity measures and valence
227 in the rhinal cortices ($maturity * valence : F(1, 32) = 0.690, p = 0.4123$) and amygdala ($maturity * valence :$
228 $F(1, 32) = 0.009, p = 0.925$) (Fig. 4B,C).

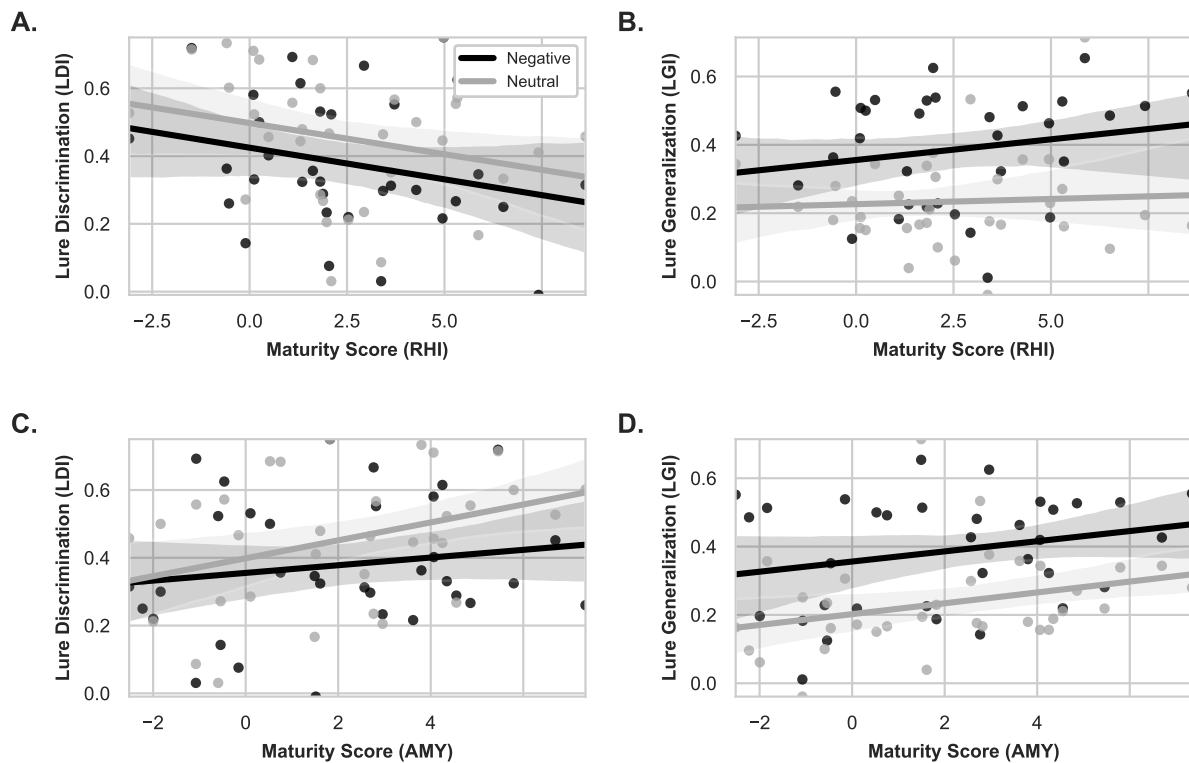


Figure 4. Rhinal cortices (RHI) and amygdala (AMY) show no differential relationship between maturity and valence with LDI and LGI performance. (A) The rhinal cortex maturity metric did not exhibit a differential relationship with discrimination for negative versus neutral valenced stimuli ($maturity * valence : F(1, 32) = 0.000, p = 0.986$) (B) nor with generalization ($maturity * valence : F(1, 32) = 0.690, p = 0.4123$). (C) The maturity metric for the amygdala similarly did not differentiate negative versus neutral stimuli for discrimination ($maturity * valence : F(1, 32) = 1.185, p = 0.284$) (D) nor generalization ($maturity * valence : F(1, 32) = 0.009, p = 0.925$) behavior.

229 **Hippocampal-mPFC anatomical connectivity exhibit trend towards differential relation be-**
230 **tween discrimination and generalization of emotionally valent stimuli**

231 We next assessed whether non-volumetric measures of maturity, in this case diffusion weighted connectivity, were
232 related to changes in discrimination and generalization with valence. We created a novel amygdala-hippocampal
233 (AMY-HF) connectivity maturity metric (see Methods) and examined the associations between this measure and image
234 valence with both LDI and LGI. We did not identify a divergence in discrimination (LDI) between negative and neutral
235 images across our AMY-HF connectivity maturity measure ($maturity * valence : F(1, 32) = 1.243, p = 0.273$)
236 (Fig. 5A). When examining generalization (LGI) we similarly did not observe a divergence in generalization with
237 image valence across changes in our AMY-HF connectivity maturity score ($maturity * valence : F(1, 32) = 0.034,$

238 $p = 0.855$) (Fig. 5B).

239 We expanded this approach to other regions sharing anatomical connectivity with the hippocampus, creating maturity
240 metrics for hippocampal-rhinal (HF-RHI) and hippocampal-mPFC (HF-mPFC) connectivity. We did not identify a
241 difference between discrimination of emotionally valent stimuli across our HF-RHI connectivity maturity measure
242 ($maturity * valence : F(1, 32) = 1.312, p = 0.260$) (Fig. 5C). When examining generalization, we did not observe
243 a divergence between emotional stimuli across our HF-RHI connectivity maturity measure ($maturity * valence :$
244 $F(1, 32) = 1.833, p = 0.186$) (Fig. 5D).

245 When examining the relationship between discrimination and generalization and our multivariate HF-mPFC anatom-
246 ical connectivity maturity measure a familiar differential pattern was evident. When comparing discrimination across
247 image valence (negative and neutral) and our HF-mPFC anatomical connectivity maturity score we observed a trend
248 towards differential discrimination ($maturity * valence : F(1, 32) = 3.885, p = 0.057$) (Fig. 6A). Generalization
249 on the other hand exhibited an inverse trend ($maturity * valence : F(1, 32) = 3.095, p = 0.088$) (Fig. 6B). These
250 trending effects mirror the interactions observed in our volumetric HF maturity analyses (Fig. 3A,C).

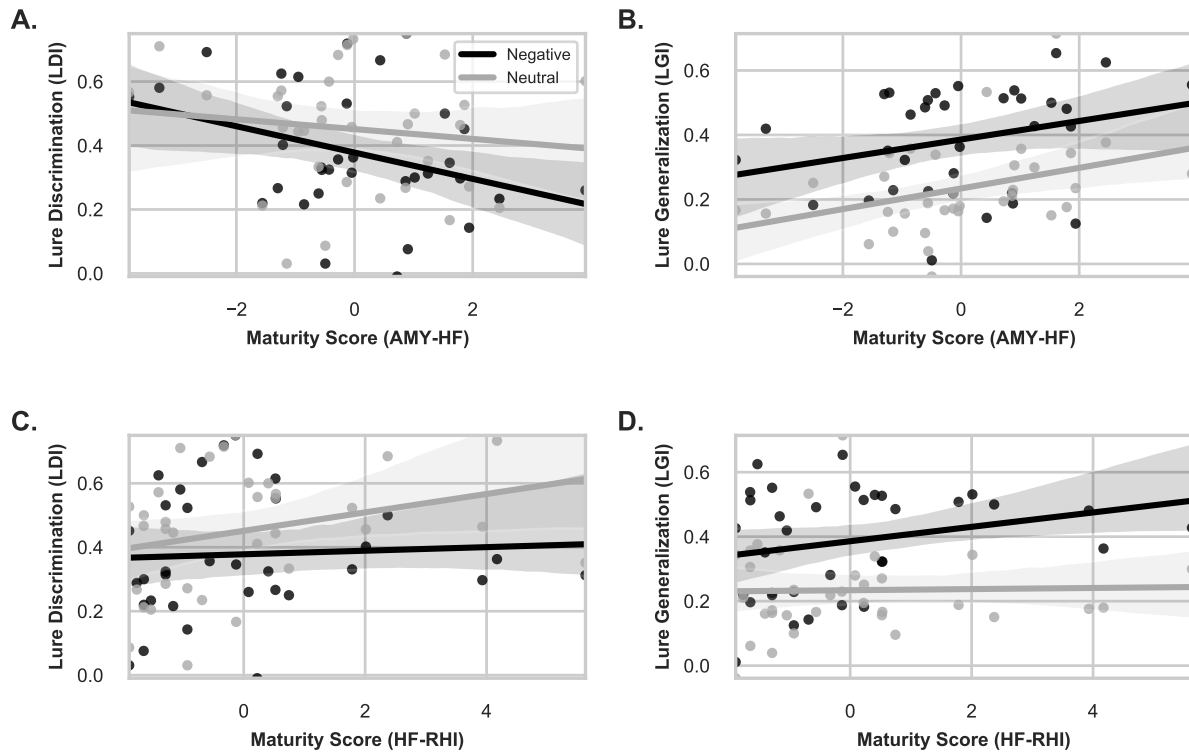


Figure 5. Association between connectivity maturity metrics and discrimination (LDI) and generalization (LGI). (A) AMY-HF connectivity maturity showed no differential relationship with LDI ($maturity * valence : F(1, 32) = 1.243, p = 0.273$) or (B) LGI ($maturity * valence : F(1, 32) = 0.034, p = 0.855$) across negative and neutral stimuli. Similarly, (C, D) HF-RHI connectivity maturity showed no valence related differential relationship with mnemonic performance (LDI: $maturity * valence : F(1, 32) = 1.312, p = 0.260$; LGI: $maturity * valence : F(1, 32) = 1.833, p = 0.186$).

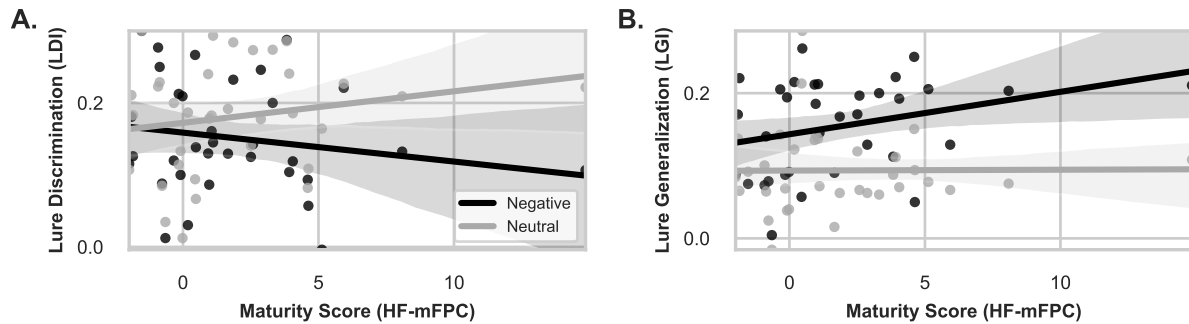


Figure 6. Maturity of HF-mPFC connectivity shows similar pattern of results to volumetric hippocampal maturity in relation to mnemonic performance. (A) There was a trending interaction between HF-mPFC connectivity and LDI ($maturity * valence : F(1, 32) = 3.885, p = 0.057$), showing increased LDI for neutral and not negative images, (B) There was evidence of a trending effect of HF-mPFC connectivity predicting LGI ($maturity * valence : F(1, 32) = 3.095, p = 0.088$).

251 Discussion

252 We examined the role of MTL maturity (defined both volumetrically and through diffusion weighted connectivity)
253 on discrimination and generalization of stimuli with emotional valence. We found greater volumetric maturity scores
254 within the HF were related to enhanced mnemonic discrimination (LDI) performance for neutral images, as well as
255 greater mnemonic generalization (LGI) for negative images. This effect of volumetric maturity appeared to be con-
256 strained to the HF and was not present in adjacent MTL regions (the amygdala and rhinal cortices). Employing the
257 same multivariate decomposition approach, but using anatomical connectivity between the HF and other regions, a
258 similar differential pattern of mnemonic generalization and discrimination across stimulus valence, while only trend-
259 ing, was evident in the connectivity between the HF and mPFC. Thus, development of the HF, assessed both volumet-
260 rically and through its connections to the mPFC, produce differential patterns of generalization and discrimination for
261 negative compared to neutral images during a sensitive developmental period. This finding may have implications for
262 our understanding of negative overgeneralization, a core feature of anxiety, which increases in prevalence during this
263 developmental window (Beesdo et al., 2009; Lissek et al., 2014). Specifically, maturational changes in how emotional
264 valence drives generalization may contribute to increasing negative overgeneralization and anxiety among vulnerable
265 youth.

266 Previous studies have found positive associations between age related changes in the brain and mnemonic discrimina-
267 tion performance for neutral stimuli. For example, discrimination of neutral objects is positively associated with
268 changes in DG/CA3 subfield volume across age (Lee et al., 2014). Similarly, greater volume of the CA2-4/DG
269 was associated with enhanced memory performance for neutral trivia information in early childhood (Riggins et al.,
270 2018). When using a multivariate decomposition derived from PLSC approach, a similar positive association between
271 mnemonic discrimination of object images with HF maturity was shown (Keresztes et al., 2018). Our data corroborate
272 these findings, showing increases in HF maturity, using PLSC derived maturity, are associated with improvements
273 in mnemonic discrimination of neutral images. The current study also extends the findings from prior work, show-
274 ing generalization of negative images is positively associated with HF maturity. Together, our results suggest that
275 discrimination and generalization behavior are impacted differentially by emotional valence across age.

276 Generalization of emotional memories is adaptive and common. Behaviorally, learning under conditions of threat
277 (Starita et al., 2019) or following negative (Schechtman et al., 2010) or aversive feedback (Resnik et al., 2011) fa-
278 cilitates generalization of episodic memories. While the amygdala has long been known to facilitate consolidation
279 (McGaugh, 2004) and recently been shown to prioritize declarative memories through its coordinated neural activity
280 with the hippocampus (Manns and Bass, 2016), damage to this region specifically impairs gist memories and leaves

281 detailed memories spared (Adolphs et al., 2001, 2005). Neurons in the amygdala have been shown to have specific
282 tuning properties related to generalization (Resnik and Paz, 2015) and specific populations in the lateral amygdala
283 signal general versus cue-specific associations (Ghosh and Chattarji, 2015). While we did not identify in our results a
284 difference in discrimination or generalization with emotional valence related to our volumetric or connectivity based
285 metrics of maturation of the amygdala, a trend in amygdala volume ($F(1, 32) = 3.679, p = 0.064$) and connectivity
286 with the HF ($F(1, 32) = 5.373, p = .027$) was associated with broad generalization irrespective of emotional valence.
287 Rather, our results provide a novel contribution to the potential mechanisms underlying generalization and suggest the
288 HF plays a unique developmental role, differentiating items to be discriminated from items garnering generalization.
289 These results support the notion that the generalization of emotional stimuli is supported by a broad network of regions
290 (Asok et al., 2019).

291 Differences in development across the HF contribute to heterogeneity of behavior well into adulthood. The HF experi-
292 ences a protracted post-natal development in primates, with histology indicating profound increases in the DG volume
293 (Lavenex et al., 2007). This protracted development has also been observed in studies of the human hippocampus
294 using structural MRI. Some studies have reported greater hippocampal volume from childhood through adolescence
295 (Ostby et al., 2009), while others have localized these changes to the hippocampal body and reported concomitant
296 decreases of volume in the head of the hippocampus (Gogtay et al., 2006; DeMaster et al., 2014). Focus on individual
297 subfields using structural MRI have identified increasing DG/CA3 volume as participants approach adolescence (Lee
298 et al., 2014; Daugherty et al., 2017). Stereological studies in macaques have similarly demonstrated that DG granule
299 cell populations mature well beyond early life (Jabès et al., 2011). Notably, the CA3 appears to mature in lock step
300 with the DG (Jabès et al., 2011). Histological studies in humans have corroborated these findings, showing increases
301 in postnatal volume across the HF marked by prolonged development of the DG and CA3, while the rhinal cortices
302 exhibit a comparatively earlier maturational plateau (Insausti et al., 2010).

303 These differences in subfield volume and trajectories across development highlight the importance of using methods
304 to simplify the input data when constructing models of HF development. This heterogeneity across the hippocampus
305 is best captured by use of multivariate decomposition techniques (Keresztes et al., 2018). Our data demonstrates that
306 findings such as those of Keresztes et al. (2018) are replicable across samples and different but related tasks using
307 such techniques. Our data also demonstrates these techniques are sensitive to region specific changes, as indicated by
308 different mnemonic outcome predictions between different constituent regions of the MTL (HF, amygdala, and rhinal
309 cortices).

310 In addition to multiple internal structures, the HF shares robust anatomical connections with the mPFC (Varela et
311 al., 2014). The mPFC contributes to schema development (van Kesteren et al., 2010) and is sensitive to information

312 congruent with previous experience (van Kesteren et al., 2010). Developmentally related differences in the detection
313 of congruence between previous and current contexts could influence generalization and discrimination behavior.
314 The mPFC also plays an important role in mnemonic control, influencing memory specificity and generalization at
315 encoding and retrieval (Xu and Südhof, 2013). When examining connectivity between the HF and mPFC using our
316 PLSC metric, we found strikingly similar results to those in the initial analysis using only intra-HF volume.

317 The transition from childhood to adolescence (“peri-puberty”) is a neurodevelopmental window when neural networks
318 associated with generalization (Bowman and Zeithamova, 2018) and emotional processing (Phelps and LeDoux, 2005)
319 undergo dynamic change. At the same time, disorders of emotion, such as anxiety increase putting youth at a higher
320 risk for escalating mental health problems (e.g. depression) in later adolescence and adulthood (Pine et al., 1998).
321 Here we provide evidence for age related brain changes in the HF associated with the discrimination of neutral and
322 generalization of negative stimuli. A developmental change in this balance may exacerbate negative overgeneralization
323 in peri-puberty and ultimately help explain rising rates of anxiety in this developmental window.

324 Our study has several important limitations. First, our study was cross sectional, rather than longitudinal, and as such
325 we can’t make any claims that these changes in volume with age are developmental in nature (Raz and Lindenberger,
326 2011). Second, HF subfields were defined using a consensus labelling approach. No harmonized protocol for HF
327 segmentation exists, but are currently being devised (Olsen et al., 2019). Lastly, the limited sample size of the current
328 study warrants caution of over interpretation and the need for replication in a larger sample.

329 Despite these limitations, our results both support and expand upon previous findings in the literature. Age related
330 volumetric changes in the HF capture differences in generalization related to emotional salience and discrimination of
331 emotionally neutral images. This difference in behavior appears unique to developmental changes in the hippocampus
332 and may be related to changes in inter-regional connectivity between the HF and mPFC. Changes to the developmen-
333 tally related balance between discrimination and generalization may support mechanisms of negative overgeneraliza-
334 tion, a common feature of anxiety disorders often taking root during this developmental period.

335 **References**

- 336 Adolphs R, Denburg NL, Tranel D (2001) The amygdala's role in long-term declarative memory for gist and detail.
337 *Behavioral neuroscience* 115:983–92.
- 338 Adolphs R, Tranel D, Buchanan TW (2005) Amygdala damage impairs emotional memory for gist but not details of
339 complex stimuli. *Nature Neuroscience* 8:512–518.
- 340 Asok A, Kandel ER, Rayman JB (2019) The neurobiology of fear generalization.
- 341 Avino TA, Barger N, Vargas MV, Carlson EL, Amaral DG, Bauman MD, Schumann CM (2018) Neuron numbers
342 increase in the human amygdala from birth to adulthood, but not in autism. *Proceedings of the National Academy*
343 *of Sciences of the United States of America* 115:3710–3715.
- 344 Bates D, Mächler M, Bolker B, Walker S (2015) Fitting linear mixed-effects models using lme4. *Journal of Statistical*
345 *Software, Articles* 67:1–48.
- 346 Beesdo K, Knappe S, Pine DS (2009) Anxiety and Anxiety Disorders in Children and Adolescents: Developmental
347 Issues and Implications for DSM-V. *The Psychiatric clinics of North America* 32:483–524.
- 348 Behrens TEJ, Berg HJ, Jbabdi S, Rushworth MFS, Woolrich MW (2007) Probabilistic diffusion tractography with
349 multiple fibre orientations: What can we gain? *NeuroImage* 34:144–55.
- 350 Behrens TE, Woolrich MW, Jenkinson M, Johansen-Berg H, Nunes RG, Clare S, Matthews PM, Brady JM, Smith SM
351 (2003) Characterization and Propagation of Uncertainty in Diffusion-Weighted MR Imaging. *Magnetic Resonance*
352 *in Medicine* 50:1077–1088.
- 353 Bennett IJ, Stark CE (2016) Mnemonic discrimination relates to perforant path integrity: An ultra-high resolution
354 diffusion tensor imaging study. *Neurobiology of Learning and Memory* 129:107–112.
- 355 Bowman CR, Zeithamova D (2018) Abstract Memory Representations in the Ventromedial Prefrontal Cortex and
356 Hippocampus Support Concept Generalization. *The Journal of Neuroscience* 38:2605 LP – 2614.
- 357 Brown ES, Kulikova A, Van Enkevort E, Nakamura A, Ivleva EI, Tustison NJ, Roberts J, Yassa MA, Choi C, Frol
358 A, Khan DA, Vazquez M, Holmes T, Malone K (2019) A randomized trial of an NMDA receptor antagonist for
359 reversing corticosteroid effects on the human hippocampus. *Neuropsychopharmacology* .
- 360 Colgin LL (2011) Oscillations and hippocampal-prefrontal synchrony.

- 361 Daugherty AM, Flinn R, Ofen N (2017) Hippocampal CA3-dentate gyrus volume uniquely linked to improvement in
362 associative memory from childhood to adulthood. *NeuroImage* 153:75–85.
- 363 DeMaster D, Pathman T, Lee JK, Ghetti S (2014) Structural Development of the Hippocampus and Episodic Memory:
364 Developmental Differences Along the Anterior/Posterior Axis. *Cerebral Cortex* 24:3036–3045.
- 365 Fischl B (2012) FreeSurfer.
- 366 Ghosh S, Chattarji S (2015) Neuronal encoding of the switch from specific to generalized fear. *Nature Neuro-*
367 *science* 18:112–120.
- 368 Giedd JN, Vaituzis AC, Hamburger SD, Lange N, Rajapakse JC, Kaysen D, Vauss YC, Rapoport JL (1996) Quan-
369 titative MRI of the temporal lobe, amygdala, and hippocampus in normal human development: Ages 4-18 years.
370 *Journal of Comparative Neurology* 366:223–230.
- 371 Gogtay N, Nugent TF, Herman DH, Ordonez A, Greenstein D, Hayashi KM, Clasen L, Toga AW, Giedd JN,
372 Rapoport JL, Thompson PM (2006) Dynamic mapping of normal human hippocampal development. *Hippocam-*
373 *pus* 16:664–672.
- 374 Goldstein FC, Mao H, Wang L, Ni C, Lah JJ, Levey AI (2009) White matter integrity and episodic memory perfor-
375 mance in mild cognitive impairment: A diffusion tensor imaging study. *Brain Imaging and Behavior* 3:132–141.
- 376 Greenberg T, Carlson JM, Cha J, Hajcak G, Mujica-Parodi LR (2013) Neural reactivity tracks fear generalization
377 gradients. *Biological Psychology* 92:2–8.
- 378 Insausti R, Cebada-Sánchez S, Marcos P (2010) *Postnatal Development of the Human Hippocampal Formation*,
379 Vol. 206 of *Advances in Anatomy, Embryology and Cell Biology* Springer Berlin Heidelberg, Berlin, Heidelberg.
- 380 Jabès A, Lavenex PB, Amaral DG, Lavenex P (2011) Postnatal development of the hippocampal formation: A stere-
381 ological study in macaque monkeys. *The Journal of Comparative Neurology* 519:1051–1070.
- 382 Jbabdi S, Sotiropoulos SN, Savio AM, Graña M, Behrens TE (2012) Model-based analysis of multishell diffusion MR
383 data for tractography: How to get over fitting problems. *Magnetic Resonance in Medicine* 68:1846–1855.
- 384 Jin J, Maren S (2015) Prefrontal-hippocampal interactions in memory and emotion.
- 385 Keresztes A, Bender AR, Bodammer NC, Lindenberger U, Shing YL, Werkle-Bergner M (2017) Hippocampal ma-
386 turity promotes memory distinctiveness in childhood and adolescence. *Proceedings of the National Academy of*
387 *Sciences of the United States of America* 114:9212–9217.

- 388 Keresztes A, Ngo CT, Lindenberger U, Werkle-Bergner M, Newcombe NS (2018) Hippocampal Maturation Drives
389 Memory from Generalization to Specificity. *Trends in Cognitive Sciences* 22:676–686.
- 390 Knierim JJ, Neunuebel JP (2016) Tracking the flow of hippocampal computation: Pattern separation, pattern comple-
391 tion, and attractor dynamics. *Neurobiology of learning and memory* 129:38–49.
- 392 Lavenex P, Banta Lavenex P (2013) Building hippocampal circuits to learn and remember: Insights into the develop-
393 ment of human memory. *Behavioural Brain Research* 254:8–21.
- 394 Lavenex P, Banta Lavenex P, Amaral DG (2007) Postnatal Development of the Primate Hippocampal Formation.
395 *Developmental Neuroscience* 29:179–192.
- 396 Leal SL, Tighe SK, Yassa MA (2014) Asymmetric effects of emotion on mnemonic interference. *Neurobiology of*
397 *Learning and Memory* 111:41–48.
- 398 Lee JK, Ekstrom AD, Ghetti S (2014) Volume of hippocampal subfields and episodic memory in childhood and
399 adolescence. *NeuroImage* 94:162–171.
- 400 Lissek S, Bradford DE, Alvarez RP, Burton P, Espensen-Sturges T, Reynolds RC, Grillon C (2014) Neural substrates
401 of classically conditioned fear-generalization in humans: a parametric fMRI study - PubMed. *Social Cognitive and*
402 *Affective Neuroscience* 9:1134–1142.
- 403 Manns JR, Bass DI (2016) The Amygdala and Prioritization of Declarative Memories. *Current Directions in Psycho-*
404 *logical Science* 25:261–265.
- 405 Marr D (1971) Simple Memory: A Theory for Archicortex. *Philosophical Transactions of the Royal Society B:*
406 *Biological Sciences* 262:23–81.
- 407 McGaugh JL (2004) The amygdala modulates the consolidation of memories of emotionally arousing experiences.
408 *Annual review of neuroscience* 27:1–28.
- 409 Mcgaugh JL, Ayala FJ (2013) Making lasting memories: Remembering the significant. *Proceedings of the National*
410 *Academy of Sciences of the United States of America* 110:10402–10407.
- 411 McIntosh AR (2000) Towards a network theory of cognition. *Neural Networks* 13:861–870.
- 412 McMakin DL, Kimbler A, Tustison NJ, Pettit JW, Mattfeld AT (2020) Negative overgeneralization is associated with
413 pattern completion in peripubertal youth. *bioRxiv* .
- 414 Olsen RK, Carr VA, Daugherty AM, La Joie R, Amaral RS, Amunts K, Augustinack JC, Bakker A, Bender AR,

- 415 Berron D, Boccardi M, Bocchetta M, Burggren AC, Chakravarty MM, Chételat G, de Flores R, DeKraaker J, Ding
416 SL, Geerlings MI, Huang Y, Insausti R, Johnson EG, Kanel P, Kedo O, Kennedy KM, Keresztes A, Lee JK, Linden-
417 berger U, Mueller SG, Mulligan EM, Ofen N, Palombo DJ, Pasquini L, Pluta J, Raz N, Rodrigue KM, Schlichting
418 ML, Lee Shing Y, Stark CE, Steve TA, Suthana NA, Wang L, Werkle-Bergner M, Yushkevich PA, Yu Q, Wisse LE
419 (2019) Progress update from the hippocampal subfields group. *Alzheimer's and Dementia: Diagnosis, Assessment
420 and Disease Monitoring* 11:439–449.
- 421 Ostby Y, Tamnes CK, Fjell AM, Westlye LT, Due-Tønnessen P, Walhovd KB (2009) Heterogeneity in subcortical
422 brain development: A structural magnetic resonance imaging study of brain maturation from 8 to 30 years. *The
423 Journal of neuroscience : the official journal of the Society for Neuroscience* 29:11772–82.
- 424 Phelps EA, LeDoux JE (2005) Contributions of the amygdala to emotion processing: From animal models to human
425 behavior.
- 426 Pine DS, Cohen P, Gurley D, Brook J, Ma Y (1998) The risk for early-adulthood anxiety and depressive disorders in
427 adolescents with anxiety and depressive disorders. *Archives of General Psychiatry* 55:56–64.
- 428 Ranganath C, Yonelinas AP, Cohen MX, Dy CJ, Tom SM, D'Esposito M (2004) Dissociable correlates of recollection
429 and familiarity within the medial temporal lobes. *Neuropsychologia* 42:2–13.
- 430 Raz N, Lindenberger U (2011) Only time will tell: Cross-sectional studies offer no solution to the age–brain–cognition
431 triangle: Comment on Salthouse (2011). *Psychological Bulletin* 137:790–795.
- 432 Resnik J, Paz R (2015) Fear generalization in the primate amygdala. *Nature Neuroscience* 18:188–190.
- 433 Resnik J, Sobel N, Paz R (2011) Auditory aversive learning increases discrimination thresholds. *Nature Neuro-
434 science* 14:791–796.
- 435 Riggins T, Geng F, Botdorf M, Canada K, Cox L, Hancock GR (2018) Protracted hippocampal development is
436 associated with age-related improvements in memory during early childhood. *NeuroImage* 174:127–137.
- 437 Rolls ET (2001) Neuronal networks, synaptic plasticity, and memory systems in primates. *books.google.com* .
- 438 Rolls ET (2013) The mechanisms for pattern completion and pattern separation in the hippocampus.
- 439 Schechtman E, Laufer O, Paz R (2010) Negative valence widens generalization of learning. *Journal of Neuro-
440 science* 30:10460–10464.
- 441 Sekeres MJ, Winocur G, Moscovitch M (2018) The hippocampus and related neocortical structures in memory trans-
442 formation.

- 443 Sinha N, Berg CN, Tustison NJ, Shaw A, Hill D, Yassa MA, Gluck MA (2018) APOE ϵ 4 status in healthy older
444 African Americans is associated with deficits in pattern separation and hippocampal hyperactivation. *Neurobiology*
445 *of Aging* 69:221–229.
- 446 Squire LR, Stark CE, Clark RE (2004) The medial temporal lobe.
- 447 Starita F, Kroes MCW, Davachi L, Phelps EA, Dunsmoor JE (2019) Threat Learning Promotes Generalization of
448 Episodic Memory. *Journal of Experimental Psychology* .
- 449 Suzuki WL, Amaral DG (1994) Perirhinal and parahippocampal cortices of the macaque monkey: Cortical afferents.
450 *The Journal of Comparative Neurology* 350:497–533.
- 451 van Kesteren MTR, Rijpkema M, Ruiter DJ, Fernández G (2010) Retrieval of associative information congruent with
452 prior knowledge is related to increased medial prefrontal activity and connectivity. *The Journal of neuroscience :*
453 *the official journal of the Society for Neuroscience* 30:15888–94.
- 454 Varela C, Kumar S, Yang JY, Wilson MA (2014) Anatomical substrates for direct interactions between hippocampus,
455 medial prefrontal cortex, and the thalamic nucleus reuniens. *Brain Structure and Function* 219:911–929.
- 456 Wang H, Yushkevich PA (2013) Multi-atlas segmentation with joint label fusion and corrective learning—an open
457 source implementation. *Frontiers in Neuroinformatics* 7.
- 458 Xu W, Südhof TC (2013) A neural circuit for memory specificity and generalization. *Science* 339:1290–1295.
- 459 Yassa MA, Stark CEL (2009) A quantitative evaluation of cross-participant registration techniques for MRI studies of
460 the medial temporal lobe. *NeuroImage* 44:319–27.
- 461 Yassa MA, Stark CE (2011) Pattern separation in the hippocampus. *Trends in Neurosciences* 34:515–525.
- 462 Yushkevich PA, Amaral RS, Augustinack JC, Bender AR, Bernstein JD, Boccardi M, Bocchetta M, Burggren AC,
463 Carr VA, Chakravarty MM, Chételat G, Daugherty AM, Davachi L, Ding SL, Ekstrom A, Geerlings MI, Hassan
464 A, Huang Y, Iglesias JE, La Joie R, Kerchner GA, LaRocque KF, Libby LA, Malykhin N, Mueller SG, Olsen RK,
465 Palombo DJ, Parekh MB, Pluta JB, Preston AR, Pruessner JC, Ranganath C, Raz N, Schlichting ML, Schoemaker
466 D, Singh S, Stark CE, Suthana N, Tompary A, Turowski MM, Van Leemput K, Wagner AD, Wang L, Winterburn
467 JL, Wisse LE, Yassa MA, Zeineh MM (2015) Quantitative comparison of 21 protocols for labeling hippocampal
468 subfields and parahippocampal subregions in in vivo MRI: Towards a harmonized segmentation protocol. *NeuroIm-*
469 *age* 111:526–541.